J Mater Sci (2012) 47:1767–1773
DOI 10.1007/s10853-011-5957-y

$BiFeO_3$-modified (Li, K, Na)(Nb, Ta)O_3 lead-free piezoelectric ceramics with temperature-stable piezoelectric property and enhanced mechanical strength

Jia-Jun Zhou · Jing-Feng Li · Xiao-Wen Zhang

Received: 12 July 2011 / Accepted: 13 September 2011 / Published online: 24 September 2011

Abstract $BiFeO_3$-modified lead-free piezoceramics $Li_{0.05}(Na_{0.515}K_{0.485})_{0.95}Nb_{0.8}Ta_{0.2}O_3$ (LKNNT) were successfully fabricated by conventional method to investigate its influences on phase structure and electricity as well as mechanical properties. A tiny amount of $BiFeO_3$ (BF) changes the phase structure of LKNNT to tetragonal and further to pseudocubic, and also effectively improves the sintering ability and densification of LKNNT which enhances the mechanical property. The LKNNT piezoceramics with the addition of 1 mol% BF has the bulk density of 5.02 g/cm^3 and an enhanced fracture strength of 142 MPa which is even higher than that of the sample of similar composition prepared by spark plasma sintering, also possesses room temperature electric properties of $d_{33}^* \sim 225$ pm/V, $k_p \sim 36.3\%$, $\varepsilon_r \sim 1140$, $\text{tg}\delta \sim 0.018$, $T_c \sim 305$ °C and $Q_m \sim 80$. The d_{33}^* remains constant up to 150 °C and the change ratio of dielectric property largely decreases over the temperature range of −50–150 °C, which can be attributed to the temperature-independent phase structure of LKNNT piezoceramics, making the ceramics as a promising candidate for actual applications.

Introduction

Lead-free piezoceramics has became a hot topic worldwide, and among them (K,Na)NbO_3 (KNN)-based ceramics are considered as one of the promising lead-free candidates for its high Curie point and good piezoelectric properties [1–5]. High piezoelectric properties with d_{33} constants up to 400 pC/N can be achieved in the KNN-based ceramics modified with Li, Ta, and Sb dopants even without textured microstructure [6–11]. Pure KNN shows perovskite structure with an orthorhombic symmetry at room temperature, which changes to tetragonal symmetry around 200 °C then to cubic phase above 400 °C. Doping Li, Ta, and/or Sb can significantly shift downward the tetragonal to orthorhombic transition point (T_{T-O}) from above 200 °C to room temperature, resulting in a state of two-phase coexistence in the Li, Ta, and/or Sb-doped KNN ceramics [11]. Nowadays, it is generally accepted that the piezoelectricity enhancement in the KNN system by doping Li, Ta, and/or Sb is mainly due to the shifting of T_{T-O}, which is called the polymorphism phase transition (PPT) effect; a state of two-phase coexistence at room temperature provides more polarization directions in the polycrystalline materials and thus enhances the piezoelectric response [12]. However, for such a modified KNN composition with enhanced electrical properties due to PPT effect, its electrical properties will decrease drastically even a small temperature deviation from T_{T-O} occurs [13].

This study was conducted under a motivation to improve the temperature stability of piezoelectricity in KNN-based ceramics. $BiFeO_3$ is a multiferroic material of rhombohedral phase at room temperature with a melting point of ~960 °C [14]. A small amount of $BiFeO_3$ was incorporated into Li/Ta-modified KNN with an optimized composition whose T_{T-O} is shifted closely to room temperature because of the following considerations. First, $BiFeO_3$ is also a lead-free ferroelectric compound with large spontaneous polarization, whose addition to KNN may favor the piezoelectricity enhancement by ferroelectric effect. Second, it was reported that a tiny amount of $BiFeO_3$ (BF) addition can change the phase structure of KNN [15],

J.-J. Zhou · J.-F. Li (✉) · X.-W. Zhang
Department of Materials Science and Engineering,
State Key Laboratory of New Ceramics and Fine Processing,
Tsinghua University, Beijing 100084, China
e-mail: jingfeng@mail.tsinghua.edu.cn

which may create a new phase boundary in the KNN–BF system to enhancement piezoelectricity. Last, previous studies revealed that $BiFeO_3$ is also an effective sintering aid for KNN ceramics [16]; reducing sintering temperature and hence suppressing the volatilization of alkali elements is technologically important for realizing the industrial applications of KNN-based ceramics.

This study shows that the temperature stability of piezoelectric properties can be greatly improved by adding only 1 mol% $BiFeO_3$ into Li/Ta-doped KNN ceramics (LKNNT) with an optimized composition of $Li_{0.05}(Na_{0.515}K_{0.485})_{0.95}Nb_{0.8}Ta_{0.2}O_3$, in which no phase transition existed from room temperature to Curie point. In addition, as a consequence of refined and dense microstructure the $BiFeO_3$-added LKNNT ceramics show higher mechanically properties than that without $BiFeO_3$ addition.

Experimental

(K,Na)NbO_3-based piezoceramics with compositions of $(1-x)\,Li_{0.05}(Na_{0.515}K_{0.485})_{0.95}Nb_{0.8}Ta_{0.2}O_3$-$xBiFeO_3$ (abbreviated as LKNNT–BF_x, $0.0 \leq x \leq 0.03$) were prepared by conventional process [15, 16]. Oxides and carbonates, Li_2CO_3 (97 wt%), K_2CO_3 (99 wt%), Na_2CO_3 (99.8 wt%), Nb_2O_5 (99.95 wt%), Ta_2O_5 (99 wt%), Fe_2O_3 (99 wt%), and Bi_2O_3 (99 wt%) were used as raw materials. The mixed powders after being weighed were milled for 24 h in ethanol using ZrO_2 balls, and then the slurry was dried and calcined at 850 °C for 5 h. The synthesized powder were ball milled again for 24 h also in ethanol and dried, after that the powders were pressed into small disks with of 10 mm in diameter, followed by cold isostatic pressing under 200 MPa. Finally, these pellets were sintered in air at an optimized temperature of 1120 °C for 2 h. After being painted with sliver electrodes, the samples were poled at 120 °C for 20 min under an electric field of 4 kV/mm in silicone oil.

Bulk densities of the samples were measured by the Archimedes method. The crystal structure of the sintered ceramics was determined by X-ray diffraction (XRD) characterization with Cu K_a radiation (Rigaku, D/Max 2500, Tokyo, Japan). The cross-sectional microstructures and thermally etched surfaces of the ceramics were observed by scanning electron microscopy (SEM, JSM6460, Tokyo, Japan). Energy dispersive X-ray spectroscopy (EDS) was also carried out to analyze the concentration of the involved elements qualitatively and quantitatively. OK, NaK, KK, NbL, TaM, FeK, and BiM lines were counted for the quantitation. The dielectric properties and loss at room temperature were measured using an Agilent 4194A precision impedance analyzer (Hewlett-Packard, Palo Alto, CA) at 1 kHz. The electric field-induced strains were measured by using an attachment onto the TF ANALYZER 1000 (aixACCT Systems GmbH, Germany) where the ferroelectricity was also measured. These measurements all involved the application of a triangular voltage waveform with a frequency of 10 Hz. Evaluation of dielectric temperature stability was carried out in a temperature-regulated chamber which was connected with Agilent 4294(Hewlett-Packard, Palo Alto, CA) at 1 kHz. Mechanical strength was evaluated using a modified small punch (MSP) method after the ceramic disks were polished to 0.50 mm thickness. More details of the MSP method can be found elsewhere [17].

Results and Discussion

Figure 1 shows the XRD patterns of the LKNNT–BF_x ceramic samples with $0.0 \leq x \leq 0.03$ in the ranges of 2θ from 20° to 60°. The XRD pattern differs with the variation of x. All the compositions have the dominant perovskite structure and the samples show the existence of impurities at the low addition of $BiFeO_3$. Relatively more impurities were observed in the LKNNT–$BF_{0.005}$ sample, which may be identified to be close to $K_4Nb_6O_{17}$ (PDF #76-0977) and $Li_{4.07}K_{5.70}Nb_{10.23}O_{30}$ (PDF #73-1229), as shown in Fig. 1a. It have been also reported that the second phases like $K_4Nb_6O_{17}$ and $Li_2K_3Nb_5O_{15}$ appear in Li-doped KNN ceramics [18]. When the addition of $BiFeO_3$ reaches 0.03, the second phase nearly disappears. A large amount of $BiFeO_3$ doping into KNN-based ceramics may influence the distribution of alkali elements which leads to the disappearance of the second phase, but the mechanism needs to be further investigated. In KNN-based ceramics, the analysis of the relative intensity of two peaks around $2\theta = 45°$ in XRD patterns is an effective method to distinguish the phase structure of ceramics that show orthorhombic and/or tetragonal symmetry at room temperature [19]. When the ceramics are of orthorhombic phase with $a = c > b$, $I_{(002)}/I_{(020)}$ equals 2 and the (002) line has a smaller Bragg angle [20]. But the $I_{(002)}/I_{(020)}$ equals 0.5 and the (002) line is also located at a smaller Bragg angle for KNN-based ceramics of tetragonal phase with $a = b < c$. An estimation of the tetragonal and orthorhombic phase ratio in KNN-based ceramics can be done by the following equation:

$$m_t \times 0.5 + m_o \times 2 = I(002)/I(020)$$
$$m_t + m_o = 1$$

where m_t denotes the ratio of tetragonal phase and m_o denotes the ratio of orthorhombic phase. The tetragonal phase ratio was 32, 58, 88% in LKNNT–BF_x piezoceramics for $x = 0.0$, $x = 0.005$, $x = 0.01$, respectively. The pure LKNNT ceramics shows the predominant orthorhombic phase and with increasing addition of BF, the phase structure

of the ceramics changes from orthorhombic to tetragonal and then to pseudocubic being analogous to a previous report [15]. When x equals 0.01, the sample shows the dominant existence of tetragonal phase at room temperature. The lattice parameters of the LKNNT–BF_x piezoceramics were calculated according to the method presented by Wang and Li [21], and the results are shown in Fig. 2. For pure LKNNT ceramics of orthorhombic phase, it has the lattice parameters of $a = c > b$ and angle $\beta > 90°$. When doped by 0.5 mol% $BiFeO_3$, the LKNNT ceramics shows the dominant existence of tetragonal phases, the lattice parameters changes to $a = b < c$ and $\beta = 90°$. When the addition of $BiFeO_3$ increases from 1 mol% to 2 mol%, the lattice parameters a and b increase, but c decreases. For LKNNT–$BF_{0.03}$ ceramics of pseducubic phase, its lattice parameters are $a = b = c = 3.96$ Å and $\beta = 90°$.

Table 1 shows the physical properties of the LKNNT–BF_x piezoceramics with $0.0 \leq x \leq 0.02$ at room temperature. The electrical properties of LKNNT piezoceramics could be enhanced by a proper addition of BF, which may be related to the enhanced densification behavior. When doped by 1 mol% BF, the LKNNT possess the best room-temperature electrical properties of $k_p \sim 36.3\%$, $\varepsilon_r \sim 1140$, $tg\delta \sim 0.018$ and $Q_m \sim 80$. The mechanical quality factor Q_m increases with the addition of BF, which is a combined result of the substitution of A^+ (Na^+, K^+ or Li^+) by Bi^{3+} and B^{5+} (Nb^{5+} or Ta^{5+}) by Fe^{3+} where the latter plays a more important role. Previous works have shown that Fe^{3+} was an acceptor to replace B-site ions and Bi^{3+} was a donor to replace A-site ions in KNN-based piezoceramics [22, 23]. When the addition of BF exceeds 1 mol%, the electrical properties of LKNNT piezoceramics deteriorate greatly. At the same time, the poling of samples became hard because of the inherently large leakage current of BF. The density of LKNNT–BF_x ceramics increases with the contents of BF

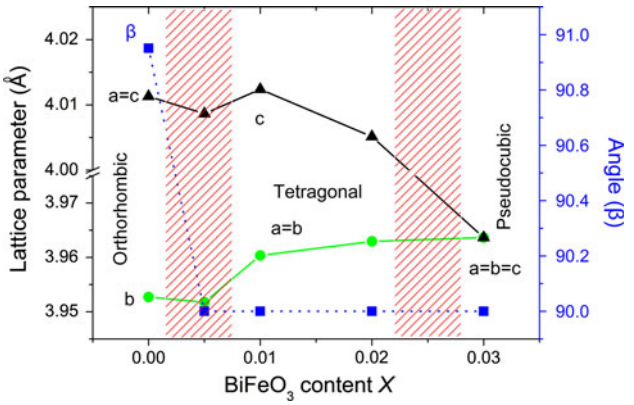

Fig. 2 Lattice parameters and angle β as a function of BF contents x for the LKNNT–BF_x ceramics

primarily and reaches the maximum of 5.02 g/cm^3 with $x = 0.01$, then decreases to 4.85 g/cm^3 for LKNNT–$BF_{0.02}$ ceramics. The variation in density is closely related to the microstructure, as shown in Fig. 3. No distinct pores are observed in LKNNT–$BF_{0.01}$ piezoceramics. The LKNNT piezoceramics possess a bimodel distribution of grain sizes which is broadened by the addition of BF. For LKNNT–$BF_{0.02}$ with excessive BF, the grains were greatly reduced to $\sim$ 500 nm. A proper addition of BF can greatly improve the sintering ability of LKNNT piezoceramics. At the same time, the elemental concentrations of all compositions were analyzed by EDS. Although EDS is not a very precise method for quantitative analysis at low concentration, the contents of Bi and Fe increase and the peaks of Fe and Bi in EDS spectrum show more and more obviously with the increase of x. Figure 4 shows the representative results of the EDS analysis for the LKNNT–BF_x piezoceramics with $x = 0.0$ and $x = 0.02$. The region enclosed by the line in the inset of the figure was analyzed, which confirmed the existence of Bi and Fe elements in the sintered samples.

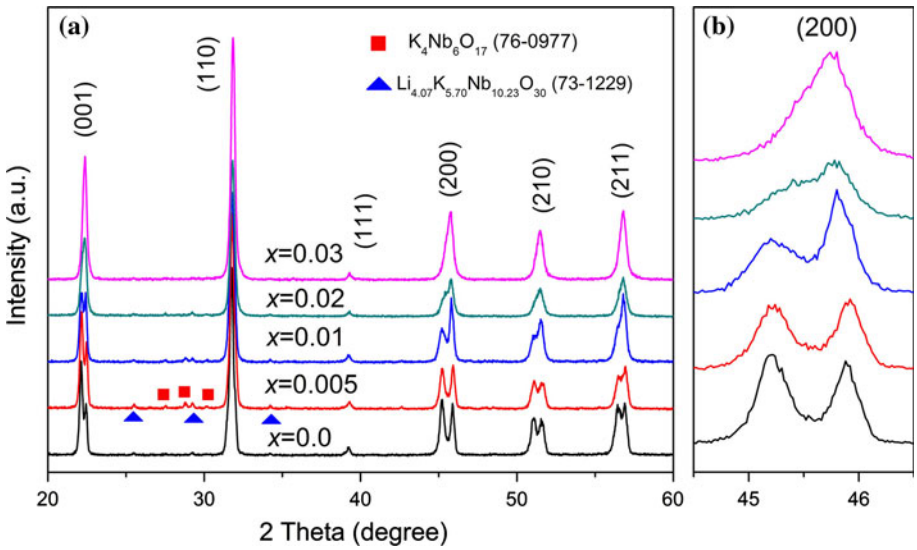

Fig. 1 XRD patterns of LKNNT–BF_x piezoceramics with $0.0 \leq x \leq 0.03$

Table 1 Physical properties of LKNNT–BF_x piezoceramics at room temperature

	$x = 0.0$	$x = 0.005$	$x = 0.01$	$x = 0.02$
ρ (g/cm^3)	4.61	4.76	5.02	4.85
k_p (%)	32.1	33.7	36.3	14.6
$\varepsilon_{33}/\varepsilon_0$	980	963	1140	858
Q_m	67	70	80	94
Loss (%)	2.5	2.1	1.8	14

Figure 5 shows the temperature dependence of the relative dielectric constant of LKNNT–BF_x ceramics which were measured at 1 kHz during the heating process, and shows that the LKNNT–$BF_{0.01}$ piezoceramics have a Curie point of 305 °C. It is hard to determine the Curie point of the pure LKNNT and LKNNT–$BF_{0.005}$ piezoceramics by the temperature dependence of dielectric constant because the relative dielectric constant will reach an abnormal value (>140000, not shown) at about 400 °C, and the mechanism need to be further investigated. The relative dielectric constant of pure LKNNT ceramics shows a peak around 30 °C (see the inset) where the polymorphism phases transition occurs. The addition of BF can decrease the T_{T-O} of LKNNT ceramics, which is similar with the addition of Bi^{3+} into KNN-based ceramics [23]; this is because the doping of Fe^{3+} to B-site of KNN has less influence on the phase structure of KNN-based ceramics as discussed in previous study [22]. At the same time, the proper addition of BF can not only increase the relative dielectric constant, but also largely decrease the change ratio of the relative dielectric constant over the temperature range from −60 to 150 °C. When the addition of BF is 1 mol%, the LKNNT piezoceramics have the most temperature stability of dielectric property.

Figure 6 displays the curves of electric-field-induced strains of LKNNT and LKNNT–$BF_{0.01}$ piezoceramics at different temperature. Although, the LKNNT–$BF_{0.01}$ piezoceramics shows a slightly lower converse piezoelectric constant d_{33}* at room temperature than LKNNT ceramics because of the shift of T_{T-O} to lower temperature by the addition of BF, but the temperature stability of the piezoelectric constant of the LKNNT–$BF_{0.01}$ is much better than the pure LKNNT ceramics. The d_{33}* of pure LKNNT

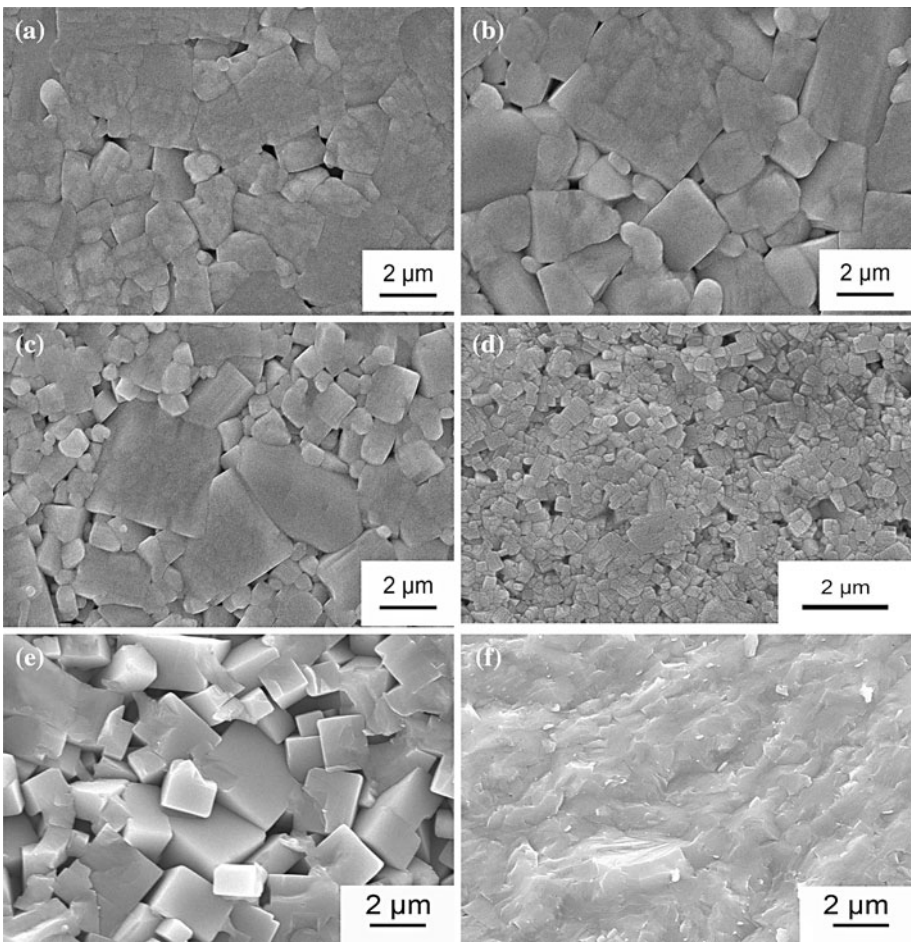

Fig. 3 SEM images of representative thermally etched surfaces (**a–d**) of LKNNT–BF_x piezoceramics: **a** $x = 0.0$, **b** $x = 0.005$, **c** $x = 0.01$, **d** $x = 0.02$, and representative fracture surfaces (**e–f**) of LKNNT–BF_x piezoceramics **e** $x = 0.0$, **f** $x = 0.01$

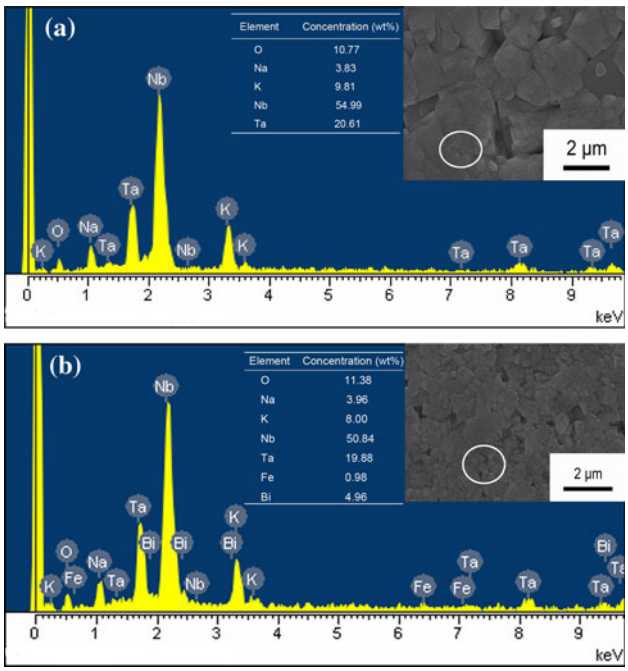

Fig. 4 Elemental concentrations of LKNNT–BF_x ceramics by EDS analysis: **a** $x = 0.0$, **b** $x = 0.02$

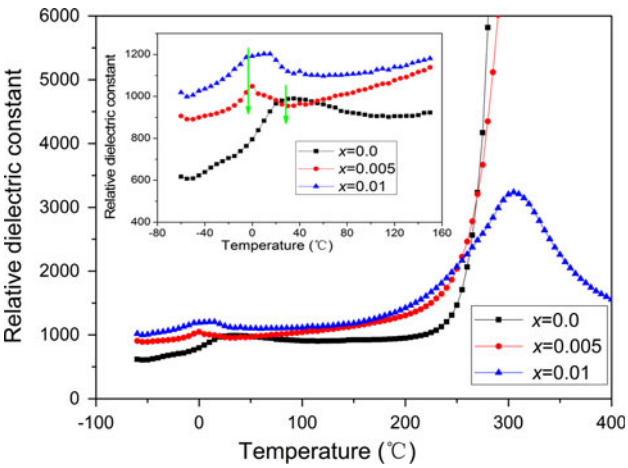

Fig. 5 Temperature dependence of the relative dielectric constant of LKNNT–BF_x ceramics with $0.0 \leq x \leq 0.01$

piezoceramics decreases from 243 to 166 pm/V as the temperature increases from 34 to 150 °C, while that of LKNNT–$BF_{0.01}$ piezoceramics nearly remain a constant value of 225 pm/V in the same temperature range. The hysteresis in the strain versus E-field behavior conducted at 34 °C is a result of domain wall movement and decreases as the temperature increases because the increased temperature could facilitate the domain wall movement. The thermal stability of piezoelectricity of LKNNT piezoceramics can be greatly improved by the doping of 1 mol% BF, which can attributed to the thermal stability of phase structure with the proper content of BF.

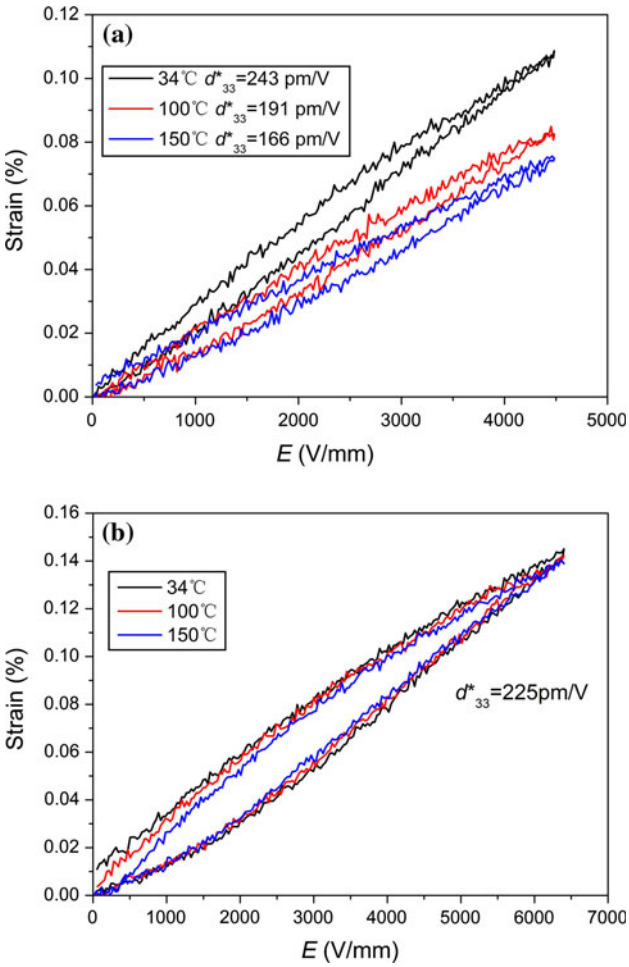

Fig. 6 Piezoelectric properties of LKNNT (**a**) and LKNNT–$BF_{0.01}$ (**b**) piezoceramics at different temperatures

Figure 7 displays the *P*–*E* loops of LKNNT and LKNNT–$BF_{0.01}$ piezoceramics measured at a frequency of 10 Hz at different temperatures. At room temperature, the LKNNT piezoceramics demonstrate a better ferroelectric property than LKNNT–$BF_{0.01}$ with a larger remnant polarization P_r of 14.3 μC/cm^2 and the lower coercive field E_c of 13.2 kV/cm, owing to the PPT effect. However, because of disappearance of the coexistence of two phases in addition to the temperature effect, the ferroelectric property of LKNNT decreases drastically with a P_r of 9.3 μC/cm^2 and 5.3 μC/cm^2 for 100 and 150 °C, respectively. Because the oxygen vacancies caused by the substitutions of Nb^{5+} by Fe^{3+} block the movement of domain wall, the LKNNT–$BF_{0.01}$ ceramics become "harder" and possess a larger coercive field E_c of 20.3 kV/cm at 34 °C. Owing to the temperature independence of phase structure of the ceramics, the P_r and E_c of LKNNT–$BF_{0.01}$ piezoceramics decrease slightly from 12.4 μC/cm^2 and 20.3 kV/cm to 9.6 μC/cm^2 and 11.5 kV/cm, respectively, as the temperature increases from 34 to 150 °C.

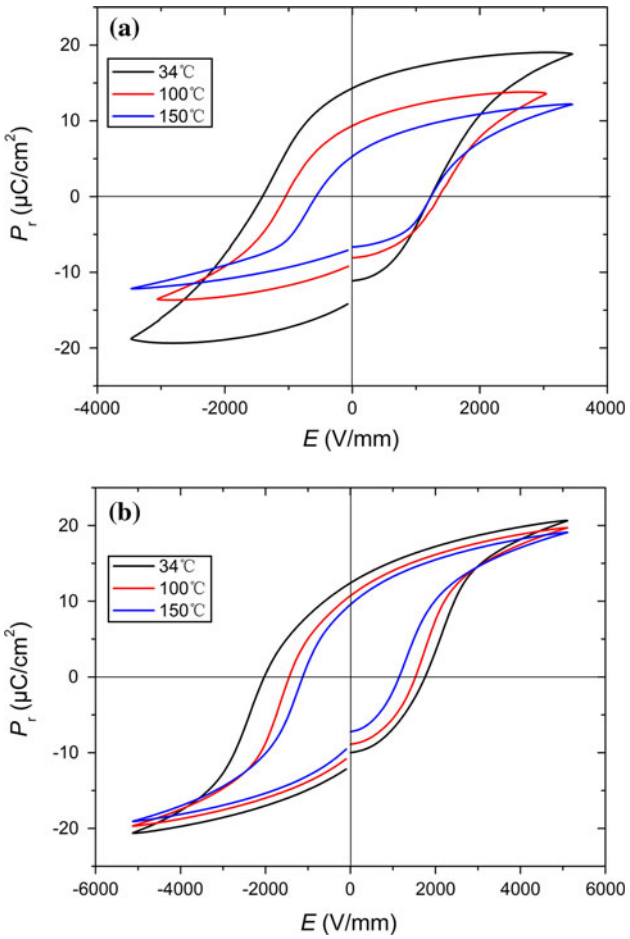

Fig. 7 Ferroelectric properties of LKNNT (**a**) and LKNNT–$BF_{0.01}$ (**b**) piezoceramics at different temperature

As shown in the Fig. 3, a proper addition of BF can decrease the grain size and improve the densification of LKNNT ceramics, which suggests the possibility to enhance the mechanical property of LKNNT piezoceramics. The measured results are shown in Fig. 8 by comparing the MSP load–displacement curves for LKNNT and LKNNT–$BF_{0.01}$ piezoceramics, which both show brittle fracture behavior. The load increases with increasing displacement and abruptly drops at a critical displacement value, which corresponds to the initiation of crack in the sample. Then with further larger displacement, the load increases to a maximum where the ultimate fracture occurs. The load when the crack initially occurs was identified as fracture load. Three samples for each composition were measured to obtain its average value. The fracture strength was calculated by the following equation:

$$\sigma_f = \frac{3P}{2\pi t^2}\left[1 - \frac{1-\gamma^2}{4} \times \frac{b^2}{a^2} + (1+\gamma)\ln\frac{a}{b}\right]$$

where $2a$ is the diameter of the load-supporting hole of the lower die here ($a = 2$ mm), $2b$ is the head diameter of the

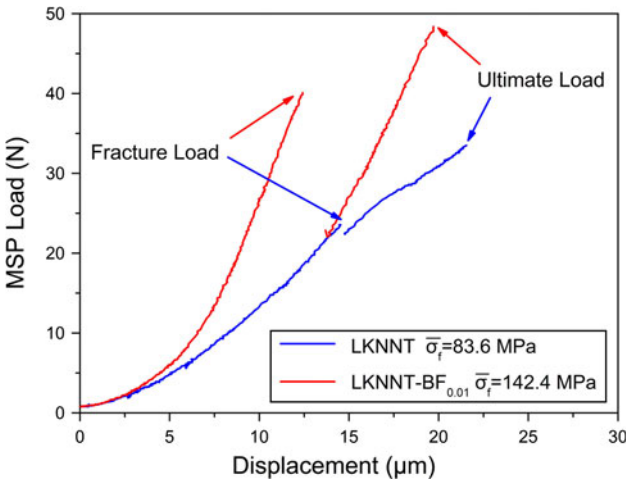

Fig. 8 MSP load–displacement curves for LKNNT and LKNNT–$BF_{0.01}$ piezoceramics

cylinder-shaped pressuring bar (here $b = 1$ mm), γ is the Poisson ratio of the tested materials (0.32), and t is the thickness of the sample ($t = 0.50$ mm), respectively. The LKNNT ceramics doped by 1 mol% BF has large average fracture strength of 142.4 MPa which is even higher than the similar composition prepared by spark plasma sintering (SPS) [17]. Although the mechanical strength of piezoelectric ceramics is often ignored, a balanced combination of mechanical and piezoelectric properties is actually important, especially for some applications where strength is important, such as bending actuators and ceramic micro-rod arrays [24]. The present LKNNT–$BF_{0.01}$ piezoceramics may be particularly suitable for such applications.

Conclusions

LKNNT–BF_x lead-free piezoceramics were prepared by conventional method to investigate the sintering behavior and temperature dependence of electric properties of the ceramics with an emphasis on the effect of $BiFeO_3$ addition. Doping 1 mol% $BiFeO_3$ can not only improve the sintering ability of LKNNT ceramics, but also shift the T_{T-O} of the ceramics to lower temperature which endows the sample with great temperature stability of electrical properties. The LKNNT–$BF_{0.01}$ piezoceramics shows much temperature-stable electric properties of $d_{33}^* \sim 225$ pm/V, $k_p \sim 36.3\%$, $\varepsilon_r \sim 1110$, $\text{tg}\delta \sim 0.018$ and $Q_m \sim 80$, and excellent mechanical property, which may meet some special requirements for practical applications.

Acknowledgements This work was supported by the Tsinghua University Initiative Scientific Research Program and the Ministry of Science and Technology of China under the Grant 2009CB623304, as

well as by National Nature Science Foundation of China (Grant Nos. 50921061 and 51028202).

References

1. Cross E (2004) Nature 432:24
2. Saito Y, Takao H, Tani T, Nonoyama T, Takatori K, Homma T, Nagaya T, Nakamura M (2004) Nature 432:84
3. Rodel J, Jo W, Seifert TPK, Anton EM, Granzow T, Damjanovic D (2009) J Am Ceram Soc 92:1153
4. Panda PK (2009) J Mater Sci 44:5049. doi:10.1007/s10853-009-3643-0
5. Shrout TR, Zhang SJ (2007) J Electroceram 19:111
6. Hollenstein E, Davis M, Damjanovic D, Setter N (2005) Appl Phys Lett 87:182905
7. Wang K, Li JF (2010) Adv Funct Mater 20:1924
8. Lin D, Kwok KW, Chan HLW (2008) Appl Phys A 91:167
9. Song HC, Cho KH, Park HY, Ahn CW, Nahm S, Uchino K, Park SH, Lee HG (2007) J Am Ceram Soc 90:1812
10. Xiao DQ, Wu JG, Wu L, Zhu JG, Yu P, Lin DM, Liao YW, Sun Y (2009) J Mater Sci 44:5408. doi:10.1007/s10853-009-3543-3
11. Gao Y, Zhang J, Qing Y, Tan Y, Zhang Z, Hao X (2011) J Am Ceram Soc. doi:10.1111/j.1551-2916.2011.04468.x
12. Dai Y, Zhang X, Zhou G (2007) Appl Phys Lett 90:262903
13. Hao J, Xu Z, Chu R, Zhang Y, Chen Q, Li G, Yin Q (2009) J Mater Sci 44:6162. doi:10.1007/s10853-009-3852-6
14. Palai R, Katiyar RS, Schmid H, Tissot P, Clark SJ, Robertson J, Redfern SAT, Catalan G, Scott JF (2008) Phys Rev B 77:014110
15. Li X, Wu L, Xiao D, Zhu J, Yu P, Jiang Y, Wu J (2008) Phys Stat Sol A 205:1211
16. Zuo R, Ye C, Fang X (2008) J Phys Chem Solids 69:230
17. Shen ZY, Zhen Y, Wang K, Li JF (2009) J Am Ceram Soc 92:1748
18. Tanaka K, Kakimoto K, Ohsato H, Iijima T (2007) Ferroelectrics 358:175
19. Guo Y, Kakimoto K, Ohsato H (2004) Appl Phys Lett 85:4121
20. Dai YJ, Zhang XW, Chen KP (2009) Appl Phys Lett 94:042905
21. Wang K, Li JF (2007) Appl Phys Lett 91:262902
22. Zuo R, Xu Z, Li L (2008) J Phys Chem Solids 69:1728
23. Du H, Liu D, Tang F, Zhu D, Zhou W, Qu S (2007) J Am Ceram Soc 90:2824
24. Shen ZY, Li JF, Chen R, Zhou Q, Shung KK (2011) J Am Ceram Soc 94:1346